Metal Oxide Nanoparticles as Bactericidal Agents

ARTICLE *in* LANGMUIR · JULY 2002

Impact Factor: 4.46 · DOI: 10.1021/la0202374

Metal Oxide Nanoparticles as Bactericidal Agents

Peter K. Stoimenov,† Rosalyn L. Klinger,† George L. Marchin,‡ and Kenneth J. Klabunde*,†

Department of Chemistry and Division of Biology, Kansas State University, Manhattan, Kansas 66506

Received March 11, 2002. In Final Form: May 20, 2002

Reactive magnesium oxide nanoparticles and halogen (Cl_2, Br_2) adducts of these MgO particles were allowed to contact certain bacteria and spore cells. Bacteriological test data, atomic force microscopy (AFM) images, and electron microscopy (TEM) images are provided, which yield insight into the biocidal action of these nanoscale materials. The tests show that these materials are very effective against Gram-positive and Gram-negative bacteria as well as spores. ζ-Potential measurements show an attractive interaction between the MgO nanoparticles and bacteria and spore cells, which is confirmed by confocal microscopy images. The AFM studies illustrate considerable changes in the cell membranes upon treatment, resulting in the death of the cells. TEM micrographs confirm these results and supply additional information about the processes inside the cells. Overall, the results presented illustrate that dry powder nanoparticulate formulations as well as water slurries are effective. It is proposed that abrasiveness, basic character, electrostatic attraction, and oxidizing power (due to the presence of active halogen) combine to promote these biocidal properties.

Introduction

Discoveries in the past decade have shown that once materials are prepared in the form of very small particles, they change significantly their physical and chemical properties, sometimes to the extent that completely new phenomena are established.[1,2] However, little is yet known about how the biological activity of a certain material changes as the size of the constituting particles decreases to nanoscale dimensions. There are some reports in the literature[3−5] that show encouraging results about the activity of different drugs and antimicrobial formulations in the form of nanoparticles. For example, Hamouda and co-workers have found[6] that specially formulated emulsions of nanosized oil droplets (nanoemulsions) demonstrate activity against bacteria and spores. Recently, it has been demonstrated that TiO_2 nanoparticles embedded in a hybrid organic/inorganic membrane can have bactericidal activity under UV-light illumination.[7]

Highly ionic nanoparticulate metal oxides are particularly interesting in that they can be prepared with extremely high surface areas and with unusual crystal morphologies that possess numerous edge/corner and other reactive surface sites.[8] Magnesium oxide prepared through an aerogel procedure (AP-MgO)[9] yields square and polyhedral shaped nanoparticles with diameters varying slightly around 4 nm, arranged in an extensive porous structure with considerable pore volume. These nanoparticles have the unique ability to destructively adsorb different gases,[10,11] including chemical warfare agents and surrogates.[11,12]

An interesting property of AP-MgO nanoparticles is their ability to adsorb and retain for a long time (on the order of months) significant amounts of elemental chlorine and bromine. AP-MgO nanoparticles can adsorb as much as 20 wt % chlorine or bromine, while common, commercially available MgO cannot adsorb more than 4 wt %.[13] It is important to note that the chemical activity of the adsorbed halogen is not reduced by being adsorbed but in fact is enhanced in some reactions.[13] Furthermore, it has been shown that AP-MgO/Cl_2 formulations are quite active as biocides, more so than free Cl_2 or AP-MgO itself or commercially available microcrystalline MgO.[14]

In this paper, we focus attention on the initial interactions, which govern the bactericidal and sporicidal activity of AP-MgO nanoparticles and their halogenated derivatives, as well as the complex surface chemistry which takes place on the bacterial membrane. Atomic force microscopy (AFM) and transmission electron microscopy (TEM) are used as complementary techniques for the investigation of the changes in the bacteria and spore cells upon nanoparticle treatment. AFM is a suitable technique for precise three-dimensional mapping of surfaces of the microbial cells and detection of very subtle changes in

* Correspondence should be addressed to K. J. Klabunde. E-mail: kenjk@ksu.edu.

† Department of Chemistry.

‡ Division of Biology.

(1) Klabunde, K. J. In *Nanoscale materials in chemistry*; Klabunde, K. J., Ed.; John Wiley and Sons: 2001 and references therein.

(2) Schmid, G. *Chem. Rev.* **1992**, *92*, 1709−1727 and references therein.

(3) Fresta, M.; Puglisi, G.; Giammona, G.; Cavallaro, G.; Micali, N.; Furneri, P. M. *J. Pharm. Sci.* **1995**, *84*, 895−902.

(4) Forestier, F.; Gerrier, P.; Chaumard, C.; Quero, A. M.; Couvreur, P.; Labarre, C. *J. Antimicrob. Chemother.* **1992**, *30*, 173−179.

(5) Couvreur, P.; Fattal, E.; Alphandary, H.; Puisieux, F.; Andremont, A. *J. Controlled Release* **1992**, *19*, 259−267.

(6) Hamouda, T.; Hayes, M.; Cao, Z.; Tonda, R.; Johnson, K.; Craig, W.; Brisker, J.; Baker, J., Jr. *J. Infect. Dis.* **1999**, *180*, 1939−1949.

(7) Kwak, S.; Kim, S. H.; Kim, S. S. *Environ. Sci. Technol.* **2001**, *35*, 2388−2394.

(8) Klabunde, K. J.; Stark, J.; Koper, O.; Mohs, C.; Park, D.; Decker, S.; Jiang, Y.; Lagadic, I.; Zhang, D. *J. Phys. Chem.* **1996**, *100*, 12142−12153.

(9) Utampanya, S.; Klabunde, K.; Schlup, J. *Chem. Mater.* **1991**, *3*, 175−181.

(10) Richards, R.; Li, W.; Decker, S.; Davidson, C.; Koper, O.; Zaikovski, V.; Volodin, A.; Rieker, T.; Klabunde, K. *J. Am. Chem. Soc.* **2000**, *122*, 4921−4925.

(11) Lucas, E.; Klabunde, K. J. *Nanostruct. Mater.* **1999**, *12*, 179−182.

(12) Wagner, G. W.; Bartram, P. W.; Koper, O.; Klabunde, K. J. *J. Phys. Chem. B* **1999**, *103*, 3225−3228.

(13) Sun, N.; Klabunde, K. J. *J. Am. Chem. Soc.* **1999**, *121*, 5587−5588.

(14) Koper, O.; Klabunde, J.; Marchin, G.; Klabunde, K.; Stoimenov, P.; Bohra, L. *Curr. Microbiol.* **2002**, *44*, 49−56.

10.1021/la0202374 CCC: $22.00
Published on Web 07/04/2002

them. TEM allows direct visualization of the morphological changes resulting in the microorganisms upon treatment.

Laser confocal microscopy is utilized to obtain information about the spatial distribution of nanoparticles and bacteria in water suspensions by imaging given areas of the sample in both transmission and fluorescent confocal modes. ζ-Potential measurements are performed to determine the charge of AP-MgO/X_2 (X = Cl, Br, none) in water suspensions. Since all microscopy techniques concentrate on a very small part of the sample, standard microbiological tests are conducted in order to estimate the overall activity of the nanoparticle compositions against certain representatives of different microorganism classes.

Experimental Section

Chemicals. Poly-L-lysine and glass disks (15 mm diameter) were obtained from Ted Pella, Inc. Mica sheets were purchased from Electron Microscopy Sciences (EMS). All electron microscopy fixatives and buffers were purchased from EMS. Ultrapure water (18.2 MΩ resistance) (Millipore Corp.) was used for all washing procedures, as well as solutions preparation.

Cultures. *Escherichia coli* strain C3000 and *Bacillus megaterium* strain ATCC14581 were obtained from ATCC. *Bacillus subtilis* ATCC6633 spores were purchased from Raven Biological Labs. *E. coli* and *B. megaterium* were grown in tryptic soy broth for 24 h before the experiment, while the spore suspension of *B. subtilis* was used as supplied.

Bacteriological Tests. Bacteriological tests were conducted as follows. Approximately 10^6 CFU (colony forming units) of bacteria or spores were deposited on water filtration membranes with pore size 0.45 μm (Millipore Corp.). The filters were dried at ambient conditions for 30 min and then completely covered with 0.25 g of AP-MgO/X_2 (X = Cl, Br, none). After 60 min, each filter was tapped to remove the powder and then transferred into a sterile Erlenmeyer flask containing 75 mL of PBS buffer and 1 wt % $Na_2S_2O_3$. The flask with the filter was shaken several times and then was left undisturbed for a total of 15 min. Three 200 μL aliquots were taken from each sample and deposited on individual Petri dishes with nutrient agar. The samples were incubated for 24 h at 37 °C and counted, and the counts on the three plates corresponding to a particular sample were averaged.

Laser Confocal Experiments. Fluorescent AP-MgO nanoparticles were prepared by mixing ~0.4 g of AP-MgO with 10 mL of 2×10^{-5} M fluorescein (Aldrich) solution in absolute methanol and shaking the mixture continuously for 20 min. The suspension was centrifuged for 5 min, and the orange sediment of AP-MgO/fluorescein was collected on the bottom. The precipitate was washed twice with absolute methanol (2 × 15 mL) to remove any residue from the fluorescein solution. After final centrifugation, the sediment was dried on a vacuum line until the pressure above the powder was lower than 1×10^{-3} Torr.

A Carl-Zeiss laser confocal microscope LSM 410 (Carl Zeiss) with an Ar−Kr gas laser was used to collect laser excited confocal and conventional transmission images using a 67× objective (1.4 numerical aperture).

ζ-Potential Measurements. The ζ-potential of the AP-MgO/X_2 in water (X = Cl, Br, none) was measured with a commercial ζ-sizer (Malvern 2C, Malvern) using NaCl as electrolyte. Two measurements were conducted at different ionic strengths (0.01 and 0.05). The samples were prepared by vigorous shaking of the corresponding powder in NaCl solution. Every reading of the instrument was recorded when consistent at least three times and averaged.

Pretreatment of the Glass Slides for AFM Studies. Glass disks were rigorously cleaned before use by submerging into 30% H_2O_2 + 98% H_2SO_4 for 1 h at 80 °C (1:4 ratio). They were washed subsequently with copious amounts of ultrapure water and finally submerged in water for at least 4 h. Part of the glass slides were treated with 10 wt % (3-aminopropyl)trimethoxysilane (Aldrich) in methanol (Fischer) for 10 min, as described previously,[15] and rinsed subsequently with copious amounts of methanol and ultrapure water.

Another portion of precleaned glass slides was covered with poly-L-lysine by applying 20 μL of the commercial 0.01 wt % solution, smeared with another glass slide, and allowed to dry. Finally, they were washed several times with ultrapure water to remove the excess polymer. These modifications of the glass support were needed to improve the adhesion of the bacteria cells. We did not find any differences between the two different support modification methods.

AFM Experiments. All samples were imaged immediately upon preparation using an atomic force microscope (Nanoscope IIIa, Digital Instruments) mounted on an inverted light microscope (100×). We used an "E" type scanner, which has a maximum scan range of 11.5 μm. All experiments were conducted in the tapping mode to avoid moving bacteria cells, as well as to minimize any physical damage to the cells by the AFM tip. OTESPA Olympus tips were 160 μm long with a typical resonant frequency of 300 kHz.

Bacteria or spore culture (10 μL) was mixed well with 10 μL of a concentrated suspension of AP-MgO/Cl_2 in water on a modified glass disk and left undisturbed for 20 min. AFM of the treated bacteria cultures was not very informative, because the bacteria cells were covered to a very high extent with the AP-MgO/X_2 (X = Cl, Br, none). To make the cells and the changes to the surface visible, treatment with a solution of HCl (0.25 M) (Fisher) and ascorbic acid (0.33 M) (Aldrich) was applied. The sample was then dried with a stream of dry air and imaged immediately.

Transmission Electron Microscopy Experiments. Approximately 10^7 bacteria or spore cells were mixed with 0.1 g of AP-MgO/X_2 powder, shaken well, and left undisturbed for 60 min. The suspension was centrifuged down to a pellet and washed twice with a mixture of HCl and ascorbic acid (0.25 and 0.33 M, respectively) to partially remove the AP-MgO/X_2 excess. All samples for the TEM were prepared following standard procedures for fixing and embedding of biological samples.[16] In the case of the spore samples, a modified fixative was used[17] to ensure fixation completeness, as well as longer periods were allowed for every step (3× those for the regular bacteria samples). The samples were cut with a diamond knife in 90−200 nm thick slices, deposited on bare 200 mesh copper grids, and stained with 2 wt % uranyl acetate, followed by 2 wt % lead citrate for 5 min each. Finally, the grids with sections were washed twice with ultrapure water. The grids were dried in a desiccator overnight and examined using a TEM Philips 201 at 80 kV accelerating potential.

Results and Discussion

As mentioned earlier, the aerogel prepared nanoparticles have very high surface areas (up to 600 m^2/g) and bear many defects, corners, and edges, which are the main contributors to their high chemical activity. The higher surface area and the higher overall reactivity of AP-MgO bring the ability to adsorb different compounds, including halogens. Halogens are well-known bactericides; however, their direct use presents many problems because of their high toxicity and high vapor pressure. The AP-MgO nanoparticles have the ability to adsorb large amounts of these (up to 20 wt %), while preserving their high activity in chemical and biological processes. This adsorption converts the halogens into an easy to handle powder form, while retaining their activity.

A. Bacteriological Tests. The bacteriological tests were conducted with three strains as representatives of different bacteria types. *E. coli* was used as an example

(15) Grabar, K. C.; Freeman, R. G.; Hommer, M. B.; Natan, M. J. *Anal. Chem.* **1995**, *67*, 735.

(16) Bechtel, D. B.; Bulla, L. A., Jr. *J. Bacteriol.* **1976**, *127*, 1472−1481.

(17) Hayat, M. A. *Fixation for electron microscopy*; Academic Press: New York, 1981.

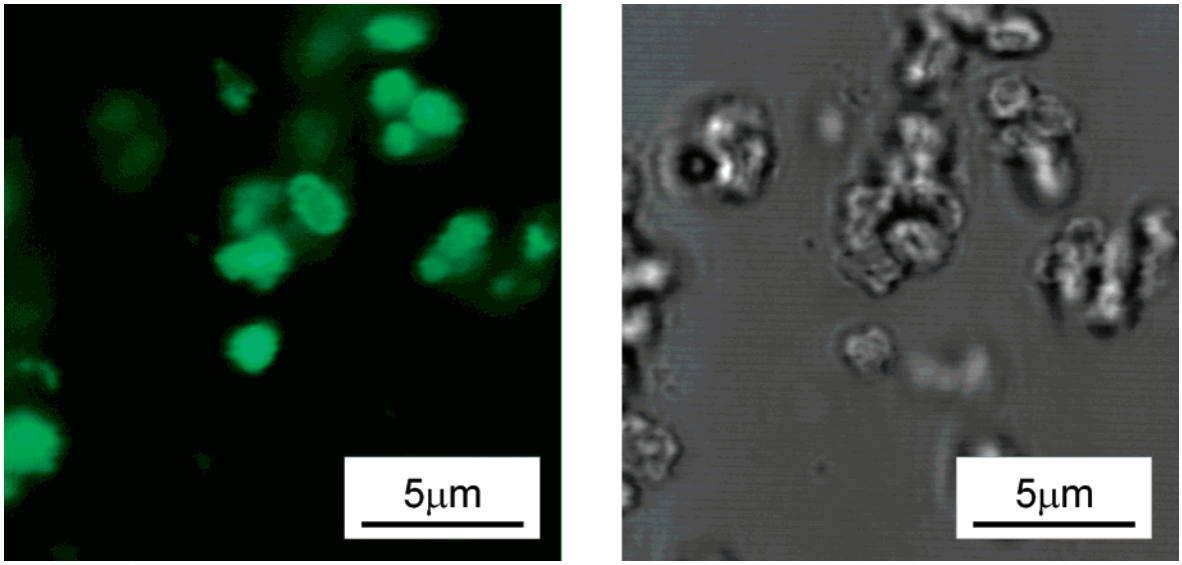

Figure 1. Confocal fluorescent (left) and transmission (right) images of *B. subtilis* spores mixed with AP-MgO/fluorescein.

for Gram-negative bacteria, *B. megaterium* was used as a representative for Gram-positive bacteria, and *B. subtilis* was used as an example of endospores. According to the test, both *E. coli* and *B. megaterium* were completely killed by any of the applied nanoparticulate formulations in 20 min or less. The spores were less susceptible to the action of the AP-MgO nanoparticles, with activity ranging from 36% (20 min) to 48% (60 min). The halogen doped powders did show significant sporicidal activity and gave results varying from 61% (20 min) up to 98% (60 min). Results were essentially identical when the same test was conducted under "wet" conditions, where a concentrated water suspension of the AP-MgO/X_2 nanoparticles was mixed directly with the corresponding bacteria cultures.

B. Confocal Laser Microscopy and ζ-Potential Measurements. We observed that an immediate coagulation occurred upon addition of AP-MgO/X_2 nanoparticles to any culture of bacteria or spores. To understand this phenomenon and localize spatially the nanoparticles, we prepared AP-MgO nanoparticles covered with a fluorescent stain. In this way we were able to take advantage of the laser confocal microscopy setup, which allows collection of images from one and the same area of the sample, while changing the type of the collected light (transmission and fluorescent), thus obtaining complementary information. By using laser light, which excites the stain, it is easier to track where the nanoparticles are spatially distributed. Bacteria and spores are not fluorescent, and they do not appear in the confocal fluorescent image. However, both the bacteria cells and the nanoparticles appear in the regular transmission image. This allows both bacteria and nanoparticles to be seen simultaneously and independently.

Confocal fluorescent and transmission images of *B. subtilis* spores mixed with AP-MgO/fluorescein from one and the same area are presented in Figure 1. The spore cells were fluorescent, indicating that they are covered by nanoparticles. It is important to note that the fluorescence is localized, while the background is practically black (nonfluorescent). Thus, we conclude that the fluorescein is firmly attached to the nanoparticles and remains attached while in the water suspension.

One can notice that in the transmission image aggregates are composed of spore cells and irregular formations (aggregates of nanoparticles). The small differences between the fluorescent and transmission images are due to the fact that the fluorescent image is collected from a single plane in the sample, while the transmission one is not confocal and contains information from other depths as well.

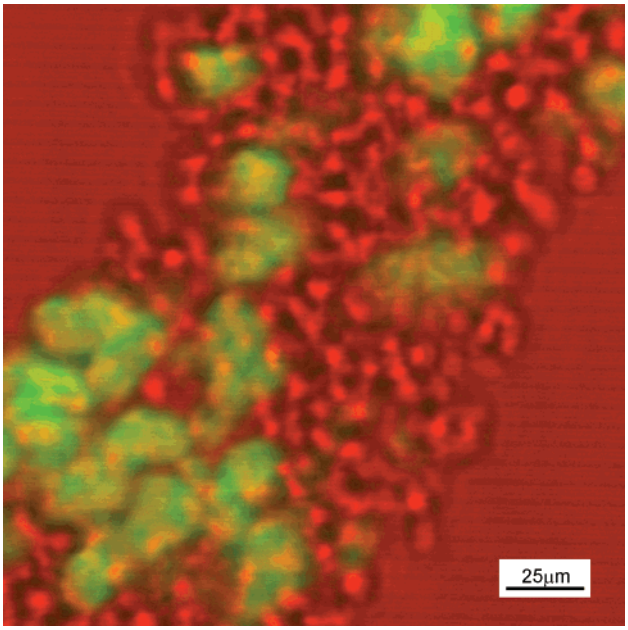

Figure 2. Simultaneous fluorescent and transmission image of *E. coli* culture mixed with AP-MgO/fluorescein (the fluorescent areas are green; the nonfluorescent areas are red).

Both bacteria strains have a strong tendency toward formation of large clumps, which upon examination appear to be both bacteria and nanoparticle aggregates coagulated together (Figure 2). We can speculate that the nanoparticles are the reason for the coagulation, because of two reasons: (1) the bacteria are composed of single cells in their culture; (2) the fluorescent nanoparticles are inside the aggregates, which means that they took part in the aggregate formation process.

The expected reason for mutual coagulation of the two colloidal solutions is an electrostatic attraction between their particles. In support of this are ζ-potential measurements showing that all AP-MgO/X_2 formulations are positively charged (27.0 mV (AP-MgO/Br_2), 33.0 mV (AP-MgO/Cl_2), and 35.2 mV (AP-MgO) at 0.01 ionic strength NaCl). In contrast, it is a well-established fact in the

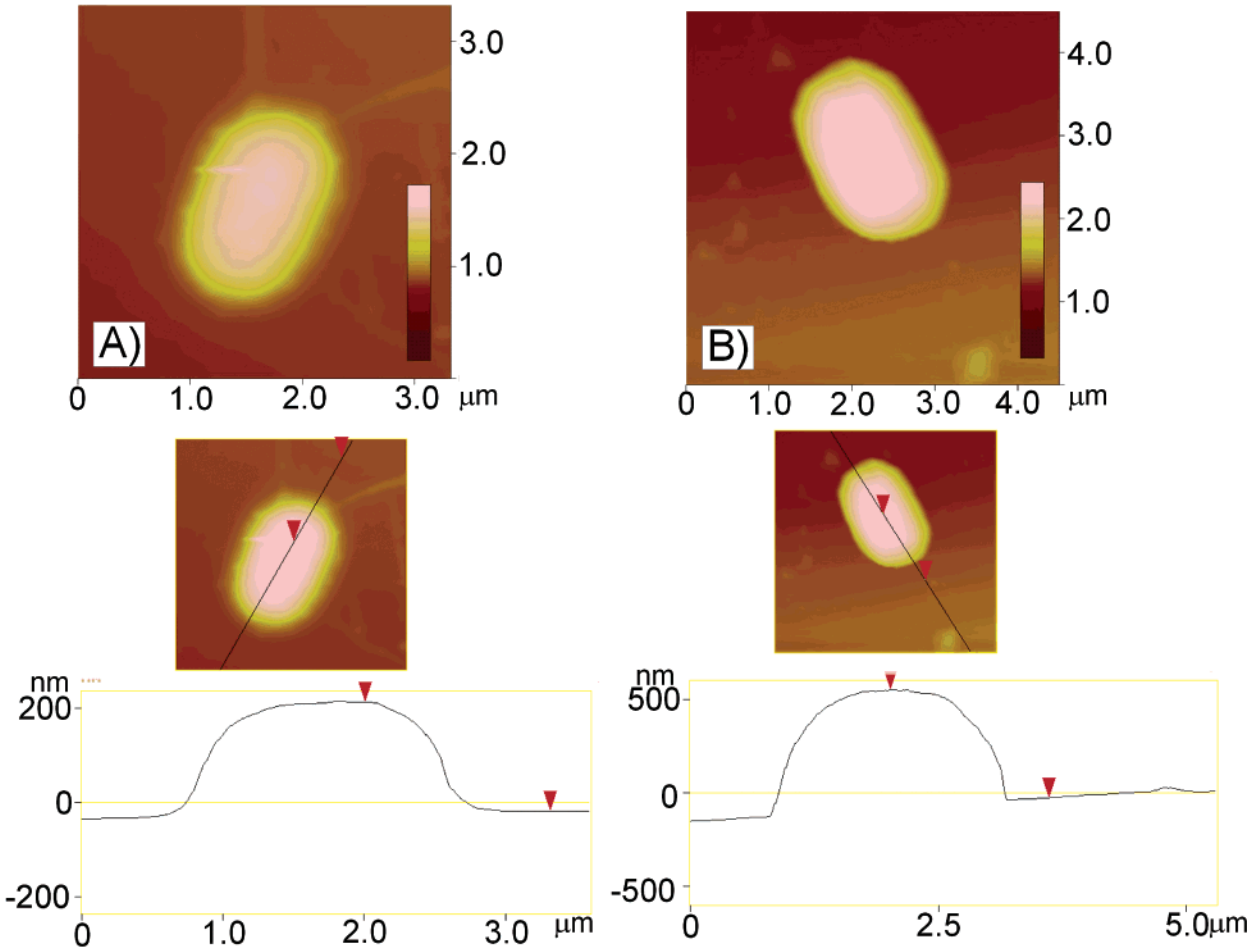

Figure 3. Tapping mode AFM images and the corresponding cross sections of (A) *E. coli* and (B) *B. subtilis* spore cells. Immediately below them are their sections. *z*-height: (A) 0−920 nm; (B) 0−630 nm.

literature[18] that the overall charge of the bacteria and spore cells at biological pH values is negative, because of the excess number of carboxylic and other groups which upon dissociation make the cell surface negative. The opposite charge of the bacteria and nanoparticles reveals one reason for the activity of the nanoparticles—they tightly bind with the bacteria surface because of electrostatic forces. Hamouda and co-workers[19] have also shown that the charge of the antimicrobial composition can be crucial for its activity. If the antimicrobial composition had the same charge as the bacteria cells, this induced repulsion and prevented the contact.[19] They found that addition of EDTA/Tris buffer to the formulation changes the charge and considerably improves the activity of the formulation.[19]

C. Atomic Force Microscopy Experiments. There are many reports[20−24] that demonstrate the suitability of atomic force microscopy for investigation of cell morphology and structure. It has been used for the investigation of animal and human cells,[20,21] as well as bacteria cells.[22−26] It appears that AFM is a very appropriate technique for elucidation of the action of bactericides on bacteria cells. Often, there are significant changes in the morphology of the cell membranes,[22−26] which can be readily observed. Indeed, the work of Camesano and co-workers[25] demonstrated that very subtle changes could be observed in the cell membrane upon treatment with different agents.

Images of *E. coli* and *B. subtilis* are shown in parts A and B of Figure 3, respectively (*B. megaterium* has not been examined with AFM because the size of the bacterium is larger than the scan range of the available scanner). Their appearance and size correspond completely with their appearance and size as measured by optical microscopy. The cross sections of the *E. coli* and *B. subtilis* cells show the corresponding height of the cells and illustrate that both cell surfaces are smooth.

Practically all *E. coli* cells were changed significantly after 20 min of treatment with AP-MgO/Cl_2 (Figure 4). The cell envelope of *E. coli* is significantly damaged upon the treatment. The cross section reveals that the smoothness and height of the cell changed dramatically as well.

(18) Busscher, H. J.; Bos, R.; van der Mei, H. C.; Handley, P. S. In *Physical Chemistry of Biological Interfaces*; Baszkin, A., Norde, W., Eds.; Marcel Dekker: New York, 2000.
(19) Hamouda, T.; Baker, J. R., Jr. *J. Appl. Microbiol.* **2000**, *89*, 397−403.
(20) Cricenti, A.; Generosi, R.; Girasole, M.; Scarselli, M.; Perfetti, P.; Bach, S.; Colizzi, V. *J. Vac. Sci. Technol. B* **1996**, *14*, 1395−1398.
(21) Girasole, M.; Cricenti, A.; Generosi, R.; Congiu-Castellano, A.; Boffi, F.; Arcovito, A.; Boumis, G.; Amiconi, G. *Appl. Phys. Lett.* **2000**, *76*, 3650−3652.
(22) Kasas, S.; Felay, B.; Carganello, R. *Surf. Interface Anal.* **1994**, *21*, 400−401.
(23) Johansen, C.; Gill, T.; Gram, L. *Appl. Environ. Microbiol.* **1996**, *62*, 1058−1064.
(24) Braga, P.; Ricci, D. *Antimicrob. Agents Chemother.* **1998**, *42*, 18−22.
(25) Camesano, T. A.; Natan, M. J.; Logan, B. E. *Langmuir* **2000**, *16*, 4563−4572.
(26) Amro, N.; Kotra, L.; Wadu-Mesthrige, K.; Bulychev, A.; Mobashery, S.; Liu, G. *Langmuir* **2000**, *16*, 2789−2796.

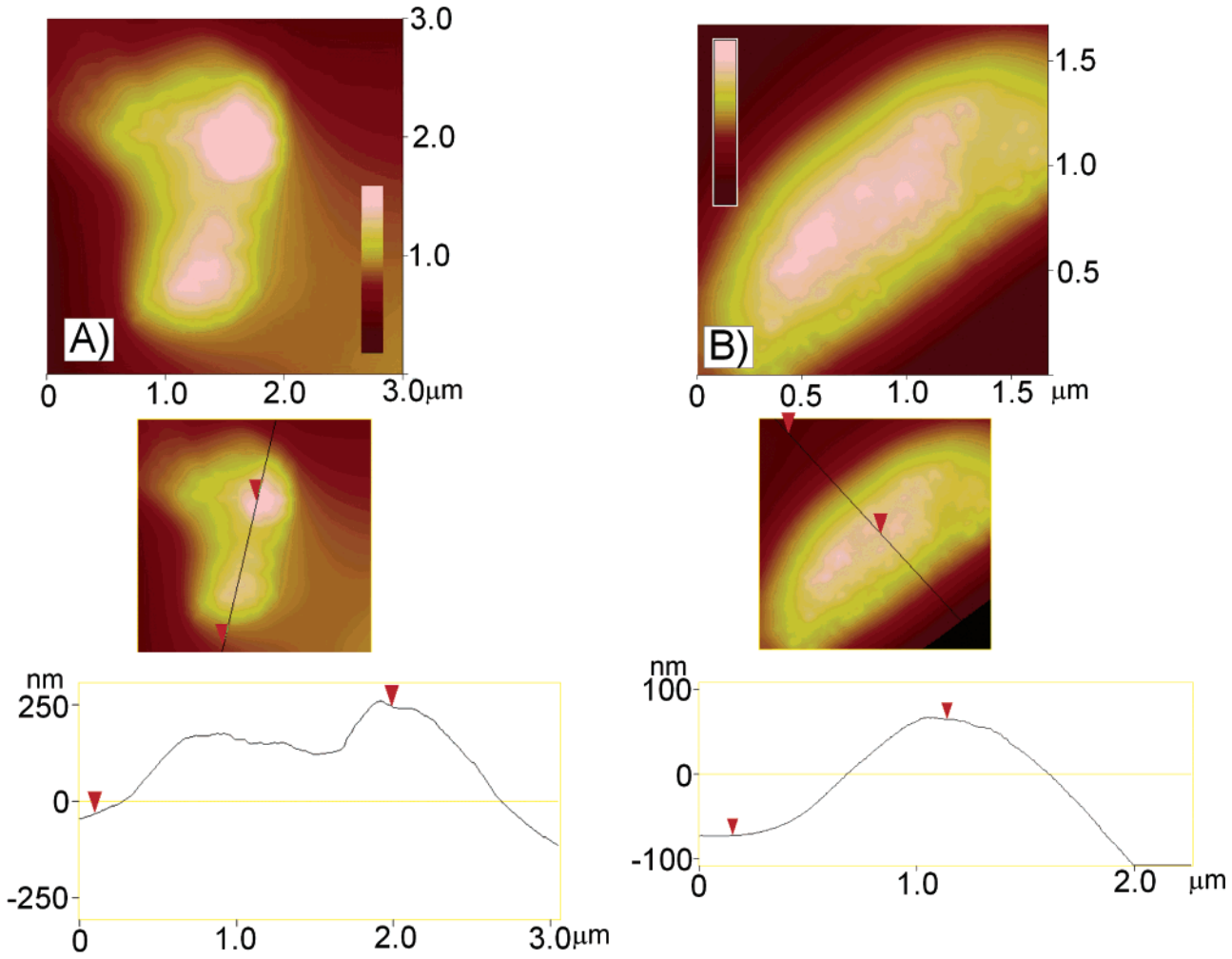

Figure 4. Tapping mode AFM images of *E. coli* treated with AP-MgO/Cl_2 for 20 min. Parts A and B are different cells found in the sample. *z*-height: (A) 0−450 nm; (B) 0−185 nm.

It seems that the nanoparticle treatment induces major damage to the cell, so eventually the cell content leaks out.

Figure 5 illustrates the AFM images of *B. subtilis* spores treated with AP-MgO/Cl_2 for 20 min. Some of the spores appear to have suffered considerable damage.

The direct interpretation of the image is that the treatment created "holes" in the cell wall, thus killing that particular spore cell. It is difficult to judge why some of the spores were damaged, while others were not. Estimation of the relative number of damaged versus not damaged spores shows that approximately 25% have a "hole". Comparison with the viability data shows excellent coincidence if it is assumed that there is one area of significant damage per cell and that the probability is 50% for the "hole" to be upward and 50% for the hole to point down. Since the atomic force microscope can image only the surface, it should observe only half of the damaged spores. In addition, the "holes" are not always on the top of the spore cell but on the borderline as well. This can be interpreted as slight "turning" of the cells and agrees with the hypothesis that some of the cells can be completely "turned around". The cross section of the damaged cell shows a significantly changed profile, increased roughness, and decreased height compared to the control (Figure 3B). The origin of the "holes" in the AFM images can be attributed to fissures, which evolve in the cell wall upon treatment. A crack in the wall would appear as a "hole" in the AFM image, because the free ends of the membrane will be free moving and much softer than the surrounding structure. Thus, when the AFM tip applies force to them, they should bend easily, causing the appearance of a depressed area.[27]

D. Transmission Electron Microscopy (TEM) Experiments. TEM is used as a complementary technique to AFM in that it examines sections of the samples. Figure 6A−C shows the TEM images of *E. coli*, *B. megaterium*, and *B. subtilis*, respectively. Characteristics of the bacteria are the well-defined cell wall as well as the evenly stained interior of the cell, which corresponds to the presence of proteins and DNA. The spore cells have very different structure, especially a much thicker and robust proteinous cell wall, which is the major barrier for the conventional bactericides.

TEM micrographs of *E. coli* treated with AP-MgO/Cl_2 show (Figure 6D) that the nanoparticles have succeeded in penetrating inside the cells, thus damaging the membranes. Practically identical results were received with AP-MgO/Br_2. AP-MgO also caused changes in the morphology of the cells; however, the effect is smaller compared to that for the halogenated formulations. These results confirm the observations from the AFM experiment that the cell membrane in all *E. coli* bacteria is extensively

(27) Weisenhorn, A.; Khorsandi, M.; Kasas, S.; Gotzos, V.; Butt, H. J. *Nanotechnology* **1993**, *4*, 106−113.

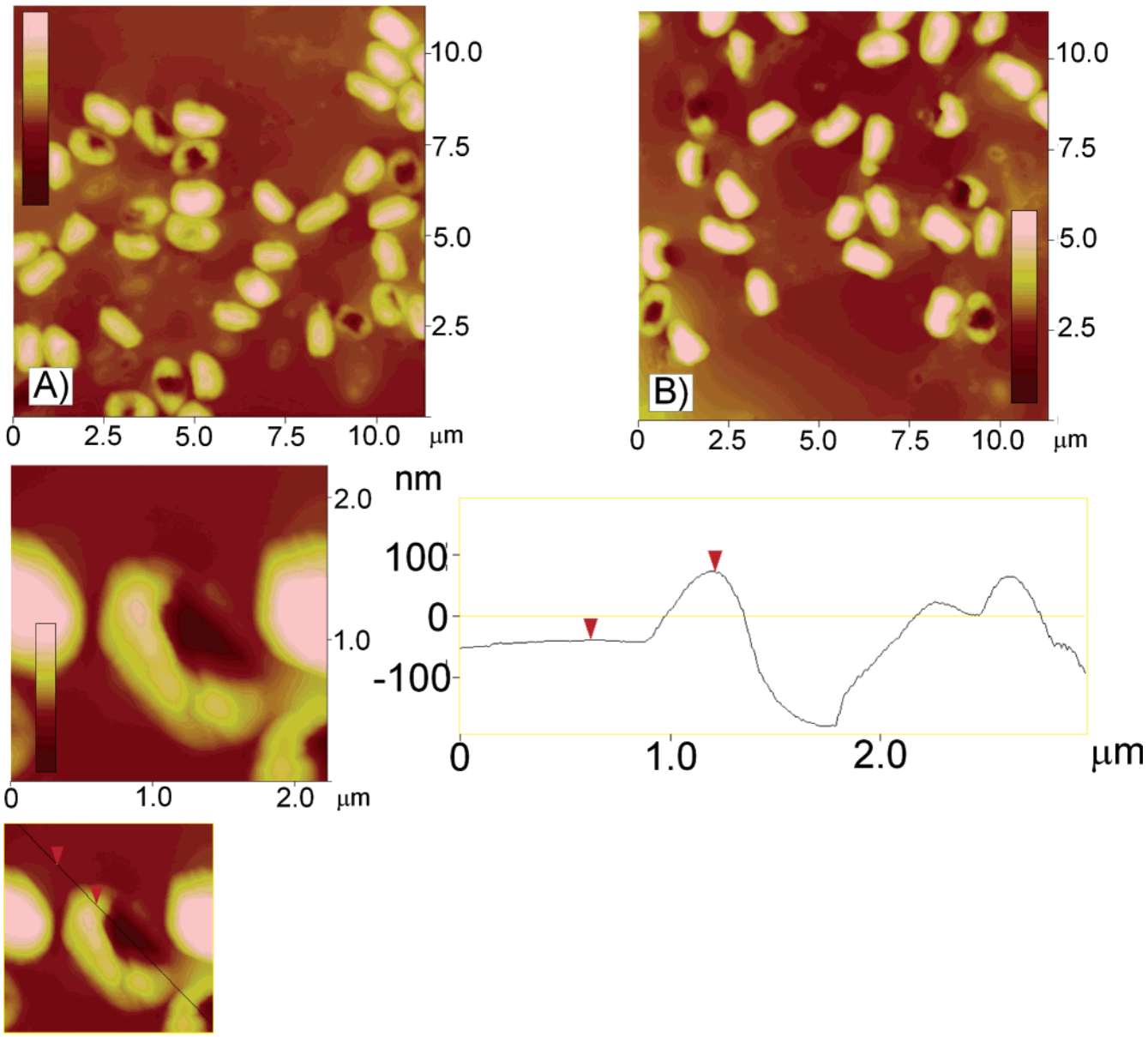

Figure 5. Tapping mode AFM images of *B. subtilis* treated with AP-MgO/Cl_2 for 20 min. Parts A and B are different areas from the sample. *z*-height: (A) 0−590 nm; (B) 0−430 nm.

damaged and, most probably, the content has leaked out. All of the cells observed had particles inside the cells. It is worth noting that the *E. coli* cells have lost the distinctiveness of the cell membrane (Figure 6E). The only observable feature for the *B. megaterium* after treatment with AP-MgO/Cl_2 or AP-MgO/Br_2 (Figure 6F) is a large number of cell membrane pieces.

The *B. subtilis* spores were significantly changed as well upon treatment. Two main types of remnants are observed—cell wall pieces (Figure 6G) and whole cell leftovers (Figure 6H and I).

From the TEM data it is apparent that the cause for the activity of the nanoparticles is in their disrupting action on the cell wall of the bacteria and spores.

Spore cells are much more robust with their thick proteinous spore coat, resulting in less than 100% killed microorganisms. They were partially killed in 20 min (the duration of the AFM experiment) and almost completely killed in 60 min (the duration of the TEM experiment).

From a chemical viewpoint, MgO is a desiccant, which can also contribute to its bactericidal activity. Nanoparticles of AP-MgO were found to be much more abrasive compared to the commercial MgO, which contributes to mechanical damage of the cell membranes.

There are reports in the literature[28−31] which show that bactericides and especially sporicides have a greatly improved efficiency when paired with alkaline substances or when the spores are pretreated with such substances. Alkaline compounds[30,31] dissolve the external part of the spore coat, which is the major protective barrier for the conventional bactericides including gaseous chlorine and bromine. AP-MgO/X_2 nanoparticles can perfectly play this "sensitizer" role, since they create an alkaline environment on their surface with adsorbed water or in an aqueous suspension.

(28) Cousins, C. M.; Allan, C. D. *J. Appl. Bacteriol.* **1967**, *30*, 168−174.
(29) Death, J. E.; Coates, D. *J. Clin. Pathol.* **1979**, *32*, 148−153.
(30) Bloomfield, S. F.; Arthur, M. *J. Appl. Bacteriol. Symp. Suppl.* **1994**, *76*, 91S−104S.
(31) Russel, A. D. In *Dissinfection, sterilization and preservation*, 4th ed.; Block, S. S., Ed.; Lea & Febiger: 1991.

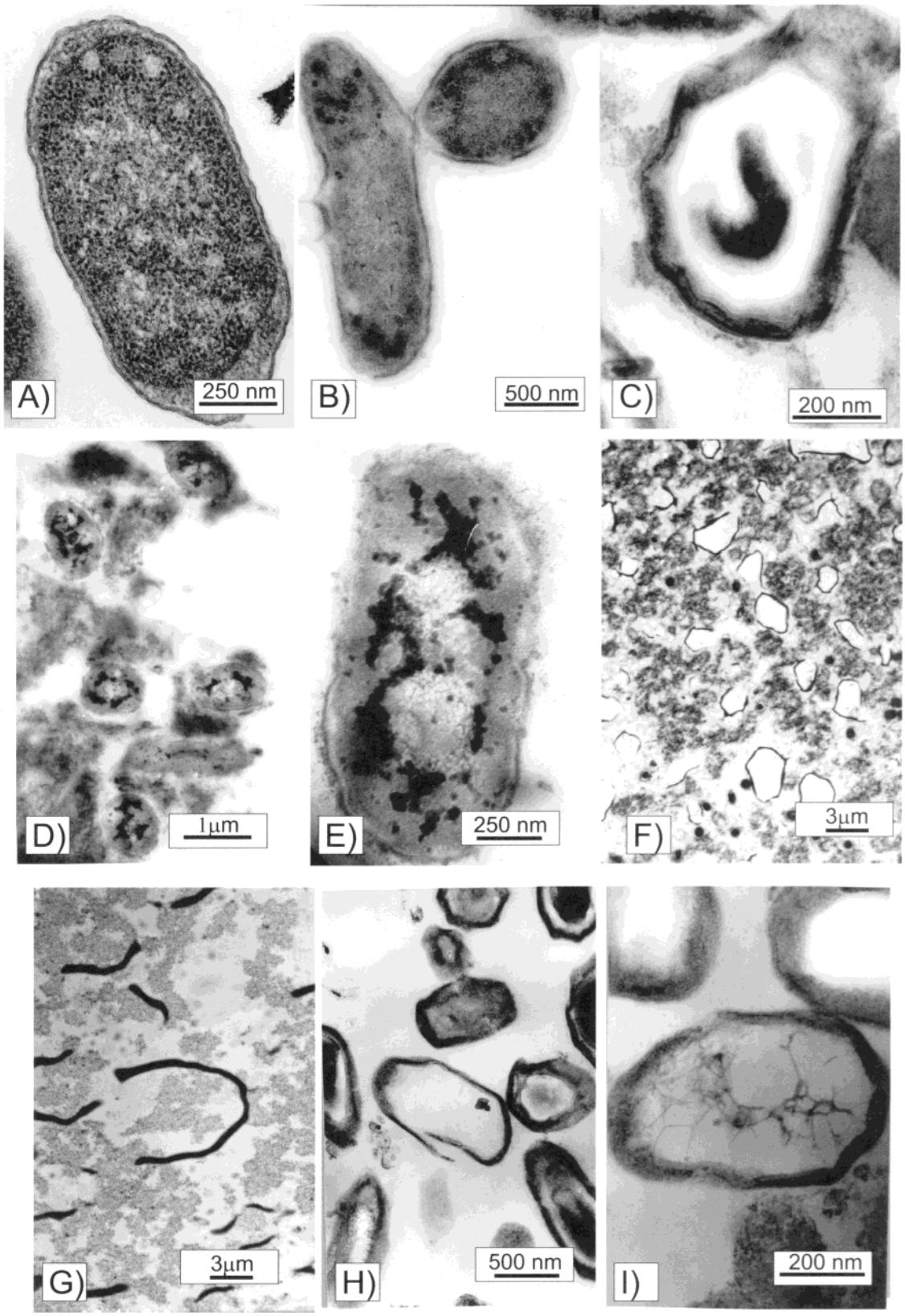

Figure 6. (A) *E. coli*—not treated; (B) *B. megaterium*—not treated; (C) *B. subtilis* spores—not treated; (D and E) TEM micrographs of *E. coli* bacteria treated with AP-MgO/Cl_2 for 60 min (AP-MgO nanoparticles appear as dark matter in the photos); (F) TEM micrograph of *B. megaterium* bacteria treated with AP-MgO/Cl_2 for 60 min; (G, H, and I) TEM micrograph of *B. subtilis* spore cells treated with AP-MgO/Cl_2 for 60 min from different areas of the grid.

Conclusions

In this paper, we present an investigation of the process by which AP-MgO/X_2 nanoparticles exhibit their biocidal action against certain Gram-positive bacteria, Gram-negative bacteria, and spore cells. AP-MgO nanoparticles are found to possess many properties that are very desirable for a potent disinfectant. Because of their very high surface area and enhanced surface reactivity, the

nanocrystals adsorb and carry a high load of active halogens. Their extremely small size allows many particles to cover the bacteria cells to a high extent and bring halogen in an active form in high concentration in proximity to the cell. Standard bacteriological tests have shown excellent activity against *E.coli* and *B. megaterium* as well as very good activity against spores from *B. subtilis*.

ζ-Potential measurements show that AP-MgO/X_2 nanoparticles have a positive charge in water suspension, opposite to those of the bacteria and spore cells, which enhances the total effect. Confocal microscopy investigation confirms that in water suspension the opposite charge brings the bacteria and nanoparticles together in aggregates composed of both AP-MgO nanoparticles and bacteria. AFM and TEM studies demonstrate that AP-MgO/X_2 has a very strong influence on microorganisms and their membranes in particular. Overall, the halogen treated MgO nanoparticles (AP-MgO/Cl_2 and AP-MgO/Br_2) were found to have a stronger and faster effect on the killing action of both bacteria and spores.

Acknowledgment. The support of Nanoscale Materials Inc. through a DARPA STTR grant and the Army Research Office through a MURI project (DAAD 19-01-1-0619) is acknowledged with gratitude. We thank Avelina Paulsen and Daniel Boyle for the assistance with the microscopy work and Olga Koper, Lisa Martin, and Kyle Knapperberger for helpful discussions.

LA0202374